

Crystal Structure and Conformational Analysis of 3 β ,17 β -Diacetoxy-8,9-seco-5 α -androsterane-8,9,11-trione

Kenji OKADA* and Hirozo KOYAMA†

Research and Development Center, Ricoh Co., Ltd., Kouhoku-ku, Yokohama 223

† Research Institute for Science and Technology, Kinki University, 3-4-1, Kowakae, Higashi Osaka 577

(Received July 26, 1993)

The crystal and molecular structures of the title compound **1** have been determined by direct methods. The crystals are monoclinic, space group $P2_1$, with $a=12.512(2)$, $b=7.436(2)$, $c=12.252(2)$ Å, $\beta=102.62(1)^\circ$, $Z=2$. The structure was refined by full-matrix least-squares calculations to a final R of 0.056 for 2268 independently observed reflections. This tricyclic compound consists of five-, six-, and ten-membered rings and is slightly bent, including two OAc side chains. The six-membered ring A has a typical chair conformation and the ten-membered ring B adopts a chair–chair conformation. Ring C is a normal β envelope. The ring junctions of both A/B and B/C are *trans* fusion. Two double bonds [C(8)=O(2), C(11)=O(4)] and two methyl groups [C(18), C(19)] of ring B are oriented α face, and one double bond [C(9)=O(3)] is on the β face of this ring. The O–C–O bond distances in the OAc side chains show partial double-bond characters.

Spectroscopic and chemical results of the title compound **1** indicated the presence of a saturated ten-membered ring (Chart 1). Our interest focused on the reactivity of this ring, ring conformation, the stereochemistry and the transannular distances of the 8-, 9-, and 11-carbonyl groups. To confirm these and to determine the geometry of the ten-membered ring, a detailed stereochemical study of **1** was undertaken. In addition, we carried out a thermal-motion analysis and a potential-energy calculation concerning the two OAc side chains for large thermal motions.

Experimental

Crystal of **1** were prepared and recrystallized from ethyl acetate as colorless prisms (mp 452–454 K). Data were collected at room temperature [295 K].

Crystal Data. $C_{23}H_{32}O_7$, $M_r=420.46$, monoclinic, $a=12.512(2)$, $b=7.436(2)$, $c=12.252(2)$ Å, $\beta=102.62(1)^\circ$, $V=1112.4(3)$ Å³. Preliminary cell data were determined from

Weissenberg and precession photographs by using Cu $K\alpha$ ($\lambda=1.5418$ Å) radiation; accurate unit-cell dimensions were obtained by a least-squares refinement of the setting angles

Table 1. Fractional Atomic Coordinates and Equivalent Isotropic Thermal Parameters^{a)} with esds in Parentheses

Atom	<i>x</i>	<i>y</i>	<i>z</i>	$B_{eq}/\text{\AA}^2$
O(1)	0.5844(3)	0.4875(0)	0.8985(2)	4.7(1)
O(2)	0.6791(2)	−0.0724(7)	0.4507(2)	4.1(1)
O(3)	0.8668(2)	0.4093(8)	0.5628(2)	4.5(1)
O(4)	0.6579(3)	0.4457(8)	0.3465(2)	4.7(1)
O(5)	0.8957(2)	0.1164(7)	0.1318(2)	3.8(1)
O(6)	0.7232(4)	0.5156(13)	1.0401(3)	12.0(4)
O(7)	1.0512(5)	0.2628(12)	0.1717(3)	13.5(4)
C(1)	0.6757(4)	0.5634(8)	0.6311(4)	3.2(2)
C(2)	0.6040(4)	0.5809(9)	0.7174(4)	3.7(2)
C(3)	0.6553(4)	0.4742(9)	0.8188(3)	3.8(2)
C(4)	0.6653(4)	0.2769(9)	0.7893(3)	3.4(2)
C(5)	0.7335(3)	0.2498(8)	0.7002(3)	2.9(1)
C(6)	0.7436(4)	0.0482(8)	0.6805(4)	3.4(2)
C(7)	0.8234(3)	−0.0075(8)	0.6076(3)	3.2(2)
C(8)	0.7741(3)	−0.0325(8)	0.4845(3)	3.1(2)
C(9)	0.7723(3)	0.3770(8)	0.5227(3)	2.9(1)
C(10)	0.6856(3)	0.3655(8)	0.5941(3)	2.7(1)
C(11)	0.7417(3)	0.3760(8)	0.3927(3)	3.2(2)
C(12)	0.8276(4)	0.3080(9)	0.3324(4)	3.4(2)
C(13)	0.8186(3)	0.1066(8)	0.3029(3)	2.7(1)
C(14)	0.8520(3)	−0.0173(8)	0.4057(3)	2.9(1)
C(15)	0.8709(4)	−0.2036(9)	0.3543(4)	3.9(2)
C(16)	0.9114(4)	−0.1549(9)	0.2475(4)	3.7(2)
C(17)	0.9119(3)	0.0494(9)	0.2460(3)	3.3(2)
C(18)	0.7073(4)	0.0661(10)	0.2279(4)	3.7(2)
C(19)	0.5745(3)	0.2941(9)	0.5307(3)	3.2(2)
C(1')	0.6280(5)	0.5173(12)	1.0036(4)	6.4(3)
C(2')	0.5405(7)	0.5311(17)	1.0711(5)	7.7(4)
C(3')	0.9723(4)	0.2190(10)	0.1063(4)	5.1(2)
C(4')	0.9487(6)	0.2675(13)	−0.0135(5)	6.0(3)

a) Anisotropically refined atoms are given in the form of the isotropic equivalent thermal parameters defined as: $B_{eq}=4/3(\sum_i \sum_j \beta_{ij} a_i \cdot a_j)$.

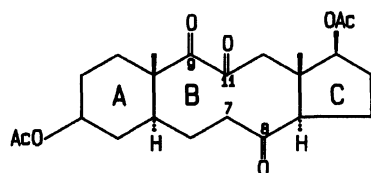


Chart 1.

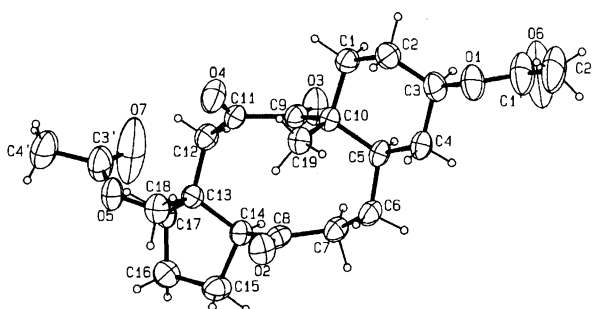


Fig. 1. ORTEP drawing¹⁹⁾ with the atomic numbering looking down the *a*-axis.

Table 2. Bond Distances (l), Angles (θ), and Torsion Angles (τ) with esds in Parentheses

(a) Bond distances/Å			
	$l/\text{\AA}$		$l/\text{\AA}$
O(1)–C(3)	1.458(6)	C(6)–C(7)	1.535(7)
O(1)–C(1')	1.303(5)	C(7)–C(8)	1.510(6)
O(2)–C(8)	1.207(5)	C(8)–C(14)	1.519(6)
O(3)–C(9)	1.201(5)	C(9)–C(10)	1.537(6)
O(4)–C(11)	1.196(6)	C(9)–C(11)	1.555(5)
O(5)–C(17)	1.457(5)	C(10)–C(19)	1.531(5)
O(5)–C(3')	1.315(7)	C(11)–C(12)	1.518(7)
O(6)–C(1')	1.177(7)	C(12)–C(13)	1.539(9)
O(7)–C(3')	1.173(7)	C(13)–C(14)	1.543(6)
C(1)–C(2)	1.534(7)	C(13)–C(17)	1.544(6)
C(1)–C(10)	1.553(8)	C(13)–C(18)	1.522(6)
C(2)–C(3)	1.495(7)	C(14)–C(15)	1.560(9)
C(3)–C(4)	1.523(9)	C(15)–C(16)	1.546(8)
C(4)–C(5)	1.539(6)	C(16)–C(17)	1.520(9)
C(5)–C(6)	1.528(9)	C(1')–C(2')	1.513(11)
C(5)–C(10)	1.565(6)	C(3')–C(4')	1.478(8)
(b) Bond angles/deg			
	$\theta/^\circ$		$\theta/^\circ$
C(3)–O(1)–C(1')	119.3(4)	O(4)–C(11)–C(9)	118.4(4)
C(17)–O(5)–C(3')	118.1(3)	O(4)–C(11)–C(12)	123.8(3)
C(2)–C(1)–C(10)	112.2(5)	C(9)–C(11)–C(12)	117.3(3)
C(1)–C(2)–C(3)	108.6(4)	C(11)–C(12)–C(13)	114.5(4)
O(1)–C(3)–C(2)	107.9(4)	C(12)–C(13)–C(14)	113.4(3)
O(1)–C(3)–C(4)	108.6(5)	C(12)–C(13)–C(17)	110.5(4)
C(2)–C(3)–C(4)	110.8(4)	C(12)–C(13)–C(18)	110.2(5)
C(3)–C(4)–C(5)	112.5(5)	C(14)–C(13)–C(17)	96.2(4)
C(4)–C(5)–C(6)	108.6(5)	C(14)–C(13)–C(18)	115.1(5)
C(4)–C(5)–C(10)	110.2(4)	C(17)–C(13)–C(18)	110.8(3)
C(6)–C(5)–C(10)	116.0(3)	C(8)–C(14)–C(13)	117.8(4)
C(5)–C(6)–C(7)	116.3(5)	C(8)–C(14)–C(15)	111.4(5)
C(6)–C(7)–C(8)	116.0(3)	C(13)–C(14)–C(15)	103.8(3)
O(2)–C(8)–C(7)	122.0(4)	C(14)–C(15)–C(16)	103.9(5)
O(2)–C(8)–C(14)	121.4(3)	C(15)–C(16)–C(17)	104.3(4)
C(7)–C(8)–C(14)	116.5(3)	O(5)–C(17)–C(13)	112.3(4)
O(3)–C(9)–C(10)	122.1(3)	O(5)–C(17)–C(16)	110.7(4)
O(3)–C(9)–C(11)	114.8(4)	C(13)–C(17)–C(16)	105.3(4)
C(10)–C(9)–C(11)	122.4(3)	O(1)–C(1')–O(6)	122.9(6)
C(1)–C(10)–C(5)	108.6(3)	O(1)–C(1')–C(2')	110.8(5)
C(1)–C(10)–C(9)	103.0(4)	O(6)–C(1')–C(2')	125.9(5)
C(1)–C(10)–C(19)	110.8(4)	O(5)–C(3')–O(7)	123.2(8)
C(5)–C(10)–C(9)	108.3(3)	O(5)–C(3')–C(4')	112.3(5)
C(5)–C(10)–C(19)	111.8(4)	O(7)–C(3')–C(4')	124.5(9)
C(9)–C(10)–C(19)	114.0(3)		

of 32 reflections ($18.2 \leq 2\theta \leq 24.6^\circ$) measured on an automatic diffractometer. Space group $P2_1$, $Z=2$, $D_x=1.256 \text{ g cm}^{-3}$, $\lambda(\text{Mo } K\alpha)=0.7107 \text{ \AA}$, $\mu(\text{Mo } K\alpha)=0.86 \text{ cm}^{-1}$, $F(000)=452$. Approximate crystal dimensions: $0.30 \times 0.35 \times 0.40 \text{ mm}$.

Data Collection and Processing. Three-dimensional intensity data were collected on a Hilger and Watts automatic four-circle Y 290 diffractometer controlled by a PDP 8 computer. The integrated intensities were measured for $2\theta < 50^\circ$ by the ω - 2θ scan technique with Zr-filtered Mo $K\alpha$ radiation and a scintillation counter. Three standard reflections (020, $13\bar{1}$, 200) were monitored every 50 reflections and showed no significant variation over the data collection. No decay corrections were applied. Thus, 2745 in-

dependent reflections ($0 \leq h \leq 16$; $0 \leq k \leq 9$; $-15 \leq l \leq 15$) were recorded, of which 2268 intensities having $I \geq \sigma(I)$ were considered to be observed. All of the intensities were corrected for the Lorentz and polarization factors, and the normalized structure factors $|E_o(\mathbf{h})|$ as well as the structure amplitudes $|F_o(\mathbf{h})|$ were derived. No absorption corrections were applied, since the specimen was considered to be sufficiently small.

Structure Analysis and Refinement. The structure was solved by a combination of direct methods with normal heavy-atom methods. The program DIRECTER¹⁾ yielded the positions for 25/30 non-hydrogen atoms of one molecule. Five other atoms were obtained from SEARCHER.¹⁾ The

Table 2. (Continued)

(c) Torsion angles/deg	$\tau/^\circ$		$\tau/^\circ$
C(10)–C(1)–C(2)–C(3)	60.9(5)	C(16)–C(17)–C(13)–C(14)	48.6(5)
C(1)–C(2)–C(3)–C(4)	–59.5(5)	C(1)–C(2)–C(3)–O(1)	–178.2(5)
C(2)–C(3)–C(4)–C(5)	58.4(6)	C(2)–C(3)–O(1)–C(1')	–135.5(6)
C(3)–C(4)–C(5)–C(10)	–54.7(5)	C(5)–C(4)–C(3)–O(1)	176.8(5)
C(4)–C(5)–C(10)–C(1)	53.1(5)	C(4)–C(3)–O(1)–C(1')	104.4(5)
C(5)–C(10)–C(1)–C(2)	–57.5(5)	C(3)–O(1)–C(1')–C(2')	178.5(5)
C(9)–C(10)–C(5)–C(6)	–71.9(5)	C(3)–O(1)–C(1')–O(6)	–8.2(5)
C(10)–C(5)–C(6)–C(7)	64.3(6)	C(6)–C(7)–C(8)–O(2)	–26.4(6)
C(5)–C(6)–C(7)–C(8)	–93.9(5)	C(15)–C(14)–C(8)–O(2)	–66.1(5)
C(6)–C(7)–C(8)–C(14)	157.7(4)	C(13)–C(14)–C(8)–O(2)	53.7(4)
C(7)–C(8)–C(14)–C(13)	–130.3(4)	C(2)–C(1)–C(10)–C(19)	65.6(4)
C(8)–C(14)–C(13)–C(12)	73.0(5)	C(19)–C(10)–C(9)–O(3)	–170.8(5)
C(14)–C(13)–C(12)–C(11)	–71.2(5)	O(3)–C(9)–C(11)–O(4)	–137.7(5)
C(13)–C(12)–C(11)–C(9)	93.1(5)	C(11)–C(12)–C(13)–C(18)	59.4(5)
C(12)–C(11)–C(9)–C(10)	–154.2(4)	C(18)–C(13)–C(17)–O(5)	49.3(4)
C(11)–C(9)–C(10)–C(5)	143.5(4)	C(15)–C(16)–C(17)–O(5)	–152.3(4)
C(17)–C(13)–C(14)–C(15)	–47.8(4)	C(13)–C(17)–O(5)–C(3')	121.9(4)
C(13)–C(14)–C(15)–C(16)	31.0(5)	C(16)–C(17)–O(5)–C(3')	–120.7(5)
C(14)–C(15)–C(16)–C(17)	–0.3(5)	C(17)–O(5)–C(3')–C(4')	176.3(5)
C(15)–C(16)–C(17)–C(13)	–30.8(5)	C(17)–O(5)–C(3')–O(7)	–2.1(5)

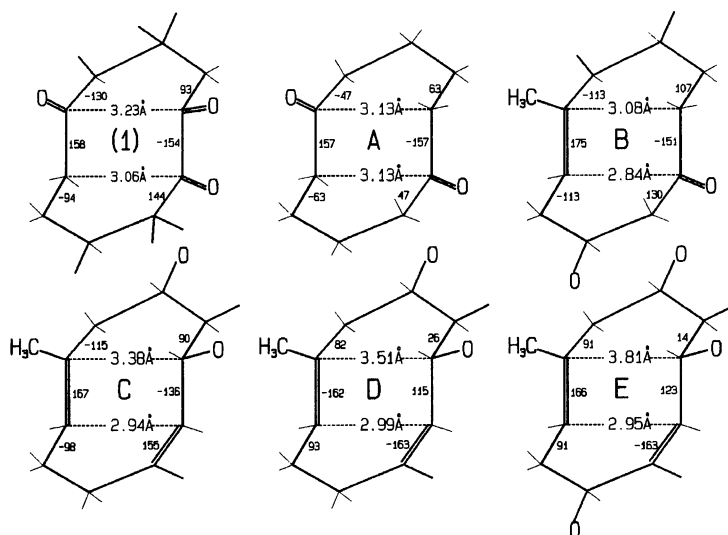


Fig. 2. Molecular conformations showing the torsion angles (in degrees) and the transannular distances (in Å): (1): 3 β , 17 β -diacetoxy-8,9-seco-5 α -androstane-8,9,11-trione (title compound), A: 1,6-cyclodecanedione,⁶⁾ B: (*E*)-3 β -(*p*-bromobenzoyloxy)-5,10-seco-1(10)-cholesten-5-one,⁸⁾ C: eupatolide,⁹⁾ D: methylhallerin,¹⁰⁾ E: ursiniolide A monohydrate.¹¹⁾

approximate coordinates were refined by full-matrix least-squares to minimized $\Sigma w[|F_o(\mathbf{h})| - |F_c(\mathbf{h})|]^2$. The 32 hydrogen atoms were located on a difference-Fourier synthesis. Inclusion of the hydrogen atoms in subsequent cycles of the least-squares refinement reduced R to 0.056, $wR=0.050$, $S=0.60(1)$ using 398 variables and $(\Delta/\sigma)_{\max}=0.31$ for 2268 reflections with $I \geq \sigma(I)$. The unit weight was applied. No further appropriate weighting scheme could be found from an analysis of the ΔF values. The max. and min. peak heights in the final difference Fourier map were 0.16 and -0.03 e \AA^{-3} . The atomic-scattering factors used in all of the calculations were taken from Ref. 2. All of the computations were performed on an NEC PC-9801RA personal computer using the DS*SYSTEM.¹⁾ The atomic coordinates are given in Table 1.³⁾

Results and Discussion

The configuration of the molecule with the atom numbering scheme is illustrated in Fig. 1. The bond distances, angles, and torsion angles are given in Table 2.

Ring A. The total ring puckering amplitude according to Cremer and Pople⁴⁾ of ring A is $Q_T = 0.594(5) \text{ \AA}$, and the puckering parameters are $q_2 = 0.035(5) \text{ \AA}$, $q_3 = -0.593(5) \text{ \AA}$, $\phi_2 = -136.5(73)^\circ$ and $\theta_2 = 176.6(5)^\circ$. The displacement asymmetry parameters according to Nardelli⁵⁾ are $D_s(C(2))=0.006(3)$ and $D_2(C(2)–C(11))=0.008(2)$. These parameters indicate a chair conformation slightly distorted from an ideal

Table 3. Analysis of the Anisotropic Displacement Parameters (ADPs) in Terms of LST Rigid-Body Motion and Internal Motions

$R_{wU} = [\Sigma w(\Delta U)^2 / \Sigma w(U_{\text{obs}})^2]^{1/2}$, where $\Delta U = U_{ij}(\text{obs}) - U_{ij}(\text{calc})$, $w = \text{reciprocal of } \sigma(U_{ij}(\text{obs}))^2$,
 $= 0.189$ (for all U s),
 $= 0.161$ (for diagonal U s only).

$\bar{\Delta}$: average differences of the mean square displacement amplitude (Δ MSDAs) (\AA^2) along the interatomic directions,
 $= 0.0129$ (for all pairs of atoms),
 $= 0.0036$ (for bonded atoms).

These values should be compared with mean esd of $U_{\text{obs}}[\bar{\sigma}(U_{\text{obs}})]$ of 0.0028, which implies an esd for Δ MSDAs of about 0.0046.

Libration		$\langle \phi^2 \rangle^{\text{a)}$	Root-mean square of the L-tensor ^{b)} eigenvalues			Root-mean square of the T-tensor ^{c)} eigenvalues		
Group	Along	(deg ²)	L_1	L_2	L_3	T_1	T_2	T_3
C(3'), C(4'), O(7)	C(17)–O(5)	189(14)	4.48	1.81	1.43	0.208	0.173	0.168
C(1'), C(2'), O(6)	C(3)–O(1)	121(23)						

a) $\langle \phi^2 \rangle$: Mean-square libration amplitudes correlations of overall and internal motion with esds. b) L-tensor: the librational tensor. c) T-tensor: the translational tensor.

Table 4. Experimental and Corrected Bond Distances (\AA) of Each OAc Side Chain

Atom	Uncorrected ^{a)}	Corrected most ^{b)}	Corrected ARGs ^{c)}	Lower bounds ^{d)}	Upper bounds ^{d)}
C(17)–O(5)	1.457(5)	1.460	1.461	1.457	1.592
O(5)–C(3')	1.315(7)	1.348	1.320	1.317	1.504
C(3')–C(4')	1.478(8)	1.482	1.482	1.478	1.704
C(3')–O(7)	1.173(7)	1.203	1.178	1.214	1.642
C(3)–O(1)	1.458(6)	1.460	1.460	1.459	1.631
O(1)–C(1')	1.303(5)	1.325	1.307	1.305	1.552
C(1')–C(2')	1.513(11)	1.515	1.515	1.513	1.790
C(1')–O(6)	1.177(7)	1.198	1.182	1.195	1.606

a) The distances between a pair of atomic positions. b) Assuming rigid motion of non-Hydrogen of the molecule. c) Assuming librational motion of rigid OAc groups about specific bonds. d) Involving hydrogen.

chair form of cyclohexane chair $|q_3| \gg q_2$ and $Q_T < 0.63 \text{ \AA}$.

Ten-Membered Ring B. Two stable conformations of ten-membered ring derivatives have been proposed⁶⁾ based on X-ray crystallographic studies. One is an extended crown conformation of approximate C_{2h} symmetry. The other has the chair form in which all of the carbon atoms of the skeleton can be distinctively grouped into three types (types I–III) with their intra/extra-annular position. A type-III atom is bonded to one intra- and one extra-annular H atom.⁷⁾ Figure 2 illustrates the interdependences of the transannular distances, torsion angles, and the steric requirements of the type-III atoms in the ten-membered ring compared with the following compounds: 1,6-cyclodecanedione (**A**),⁶⁾ (*E*)-3 β -(*p*-bromobenzyloxy)-5,10-seco-1(10)-cholesten-5-one (**B**),⁸⁾ eupatolide (**C**),⁹⁾ methylhallerin (**D**),¹⁰⁾ and ursiniolide A monohydrate (**E**).¹¹⁾ In the title compound **1** C(7) and the keto-carbon atoms [C(8), C(9), C(11)] are in the type-III positions. Oxygen atoms occur preferentially at type-III positions, since removing a type-III intra-annular H atom produces a large decrease in the strain energy. Due to the effect of removing

the transannular H...H, the transannular distances, C(7)...C(9) and C(8)...C(9) are short [3.061(5) and 3.081(4) \AA , respectively] compared with the sum of the van der Waals radii [3.10 \AA for C...C]. These short distances correspond so as to cause slight alterations in the torsion angles $\omega^{6-7}/\omega^{11-12}$, $\omega^{7-8}/\omega^{9-11}$, and $\omega^{8-14}/\omega^{9-10}$. It probably corresponds to the weak transannular bonding [C(7)_{sp³}...C(9)_{sp²} and C(8)_{sp²}...C(9)_{sp²}] associated with an $n:\pi^*$ interaction. The same tendencies are found in compounds **B–E**. The maximum deviations of the least-squares planes I[C(6), C(7), C(9), C(10)], II[C(7), C(8), C(9), C(11)], and III[C(8), C(11), C(12), C(14)] are 0.068(3), 0.070(3), and 0.003(3) \AA , respectively. Each four atoms are almost coplanar. The dihedral angles between these planes (I/II, II/III, and I/III) are 60.0(3), 59.9(3), and 4.8(2) $^\circ$, respectively. The ring puckering and displacement asymmetry parameters of ring B are $Q_T = 1.034(4) \text{ \AA}$, $D_s(\text{C}(8)) = 0.081(1)$, and $D_2(\text{C}(6)–\text{C}(5)) = 0.052(1)$. These indicate that the ten-membered ring B adopts a chair–chair conformation.

Ring C. Four atoms [C(14), C(15), C(16), C(17)] of ring C are coplanar to a standard deviation of 0.004 \AA . The maximum distortion of the bond an-

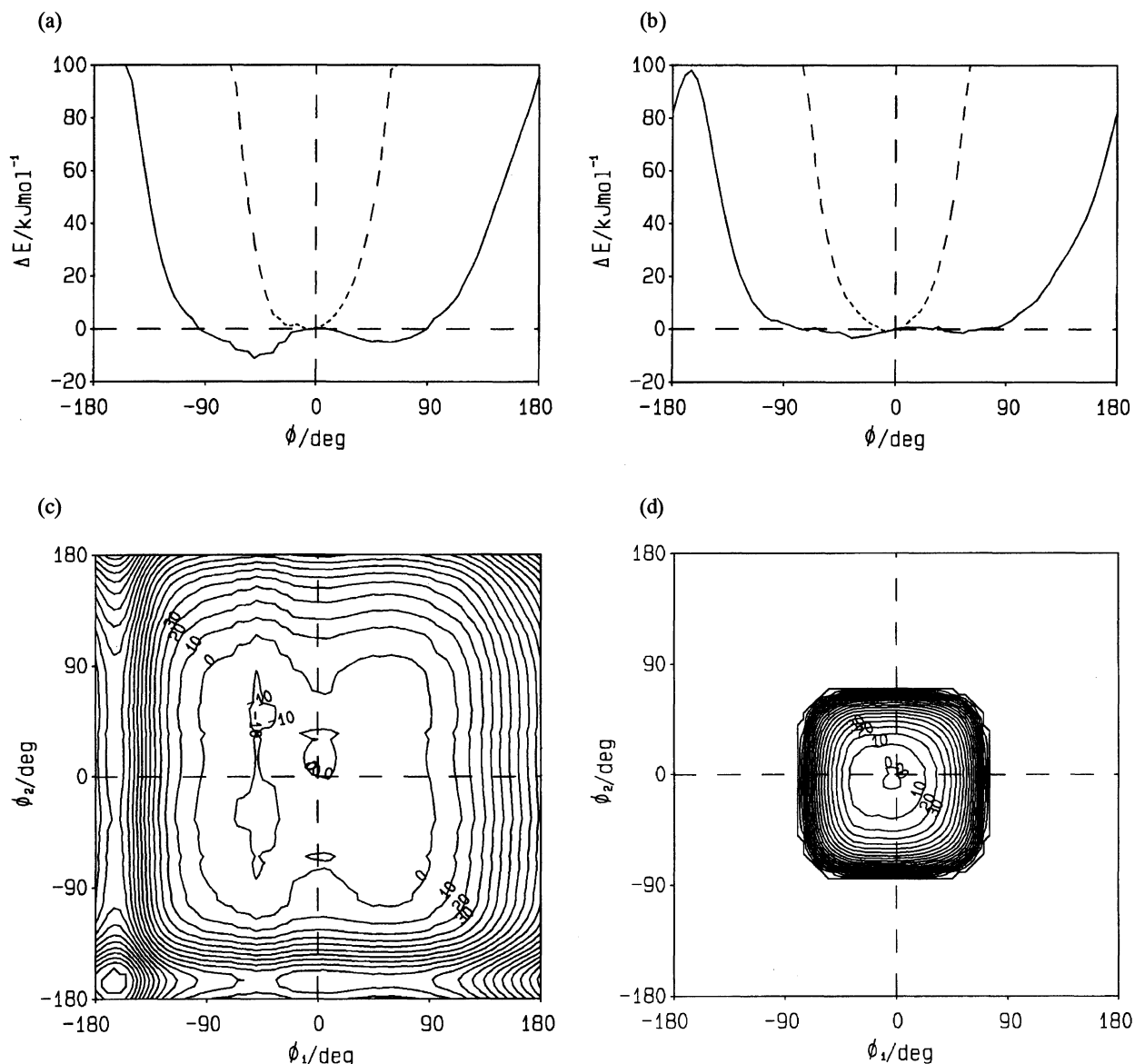


Fig. 3. Calculated difference potential-energy profiles (ΔE) and contour lines for the rotation of each OAc side chain. (a) Rotation about C(17)-O(5) (solid lines) and O(5)-C(3') (dashed lines); (b) Rotation about C(3)-O(1) (solid lines) and O(1)-C(1') (dashed lines); (c) Concomitant rotations about C(17)-O(5) (ϕ_1) and C(3)-O(1) (ϕ_2); (d) Concomitant rotations about O(5)-C(3') (ϕ_1) and O(1)-C(1') (ϕ_2). Contour lines are at 10 kJ mol^{-1} intervals. The zero of the energy is assumed for the conformation in the crystal. The counter-clockwise rotations are assumed as positive.

gles occurs at C(13) in this ring, where C(14)-C(13)-C(17) is $96.2(4)^\circ$. Atom C(13) is disposed by $0.77(1) \text{ \AA}$ from the mean plane of this ring, and especially shows a departure from the tetrahedral conformation. The ring puckering and displacement asymmetry parameters [$q_2 = 0.507(4) \text{ \AA}$, $\theta_2 = 0.8(6)^\circ$, $D_2(\text{C}(16)) = 0.088(2)$, and $D_s(\text{C}(13)) = 0.004(3)$] of ring C indicate a pure envelope conformation with the apex at C(13).

Two OAc Side Chains. The large ellipsoids at O(6) and O(7) of Fig. 1 indicate a great degree of dynamic or static disorder in that region. To confirm these, a thermal-motion analysis of the anisotropic displacement

parameters (ADPs) was carried out in terms of the **LST** rigid-body approximation according to Schomaker and Trueblood¹²⁾ as well as Trueblood,¹³⁾ while also considering the correlations in the internal and overall motions according to Dunitz and White¹⁴⁾ using the program THMA14.¹⁵⁾ Table 3 lists the ADPs for the two attached OAc rigid groups (ARGs). As can be seen from the large $\langle \phi^2 \rangle$ values, the small **L** of the ARGs and the short distances, two of the OAc atomic displacements are more pronounced, and the internal motions have some relevance, particularly for these terminals. An inspection of Fig. 1 and Table 3 suggests that a dis-

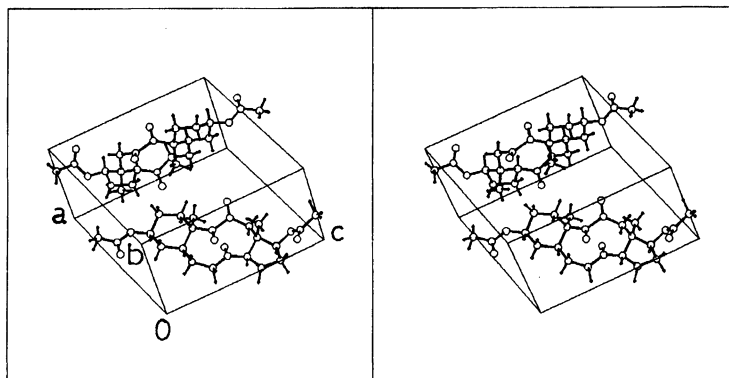


Fig. 4. Stereoscopic view of the molecular packing in the unit cell. The origin is at the lower-middle corner, the *a*-axis is horizontal and the *c*-axis is vertical.

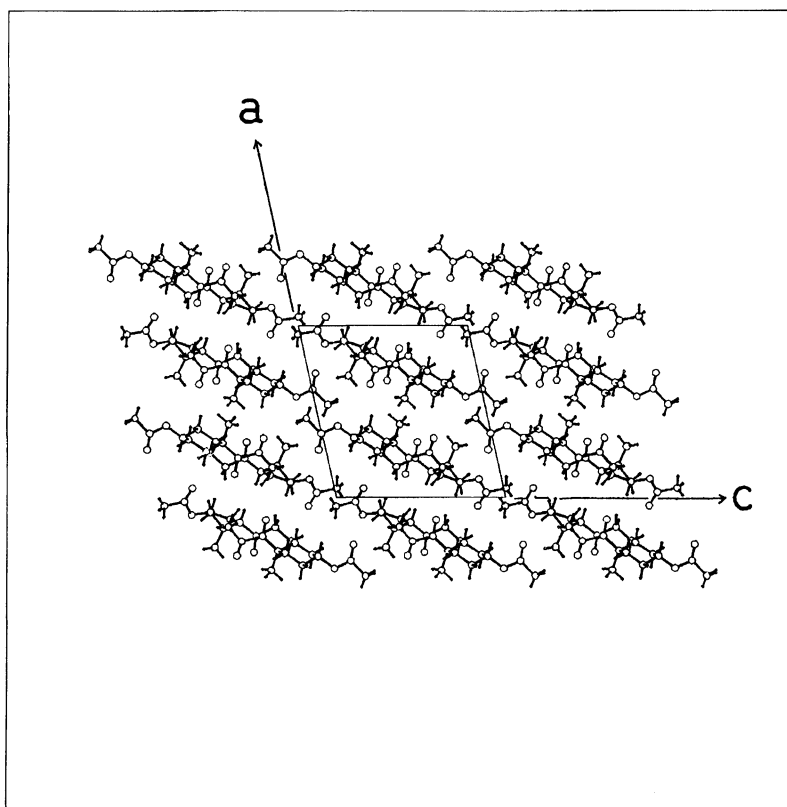


Fig. 5. Molecular packing diagram looking down the *b*-axis. The axes orientations are the same as in Fig. 4.

order should be considered around each OAc, although no significant peaks appear in the difference map. The corrected bond distances according to the two methods and the bounds following Busing and Levy¹⁶⁾ were calculated as shown in Table 4. Although the uncorrected bond lengths tend to become shorter, fairly constant values were obtained by appropriate corrections. The C(3')=O(7) and C(1')=O(6) distances of the corrected ARGs are shorter than the lower bounds. The most corrected bond lengths of each Ac are only longer than the corrected ARGs. Atom-atom nonbonded potential energy calculations were also carried out with the program ROTENER,¹⁷⁾ which makes use of a function of the type $E_{ij} = -A_{ij}r_{ij}^{-6} + B_{ij}\exp(-C_{ij}r_{ij})$. The

atomic charges are according to the method of Gasteiger and Marsili.¹⁸⁾ We assumed that there is no geometrical change during rotation of the fragment and no Coulombic energy. Figure 3 shows the curves and contour lines of nonbonded potential energies as calculated from the free molecules. The energy values are relative to the energy corresponding to the observed conformation in the crystal. The energy barriers about the O(5)-C(3') and O(1)-C(1') directions are high due to a steric hindrance caused by the hydrogen atoms of the methyl group. On the other hand, the conformations of the two OAc side chains correspond to points very wide to the minima of van der Waals potential energy upon rotation of each OAc about the C(17)-O(5) and C(3)-

O(1) directions, respectively. The two OAc conformations are not coincident with the potential-energy minimum [-50° , $\Delta E = -11.1$; -30° , $\Delta E = -3.1$ kJ mol $^{-1}$, respectively]. However, the energies between -90° to 90° have close values with the isolated molecule [2307.1 kJ mol $^{-1}$]. The contour lines indicate that quite severe steric interactions occur upon rotation of the Ac, and that no interactions occur upon rotation of the OAc. These energy calculations suggest that each OAc vibrates centering around C(17)–O(5) and in the C(3)–O(1) direction, respectively. Thus, this analysis shows that the O–C–O bond distances indicate partial double-bond interactions.

Crystal Packing. The stereo crystal-packing diagrams of **1** in a unit cell and the molecular packing diagram are shown in Figs. 4 and 5, respectively. Two molecules in a unit cell, which are related by the 2_1 axis at $(\frac{1}{2}, y, \frac{1}{2})$, are bounded to each other by van der Waals contacts. The molecule is arranged in a parallel fashion along the diagonal line through the a - and c -axes. Short contacts are: O(2)···C(19) $(1-x, -\frac{1}{2}+y, 1-z)$ 3.380(6) Å, O(3)···C(16) $(2-x, \frac{1}{2}+y, 1-z)$ 3.242(10) Å, O(6)···C(4') $(x, y, 1+z)$ 3.550(16) Å, and O(7)···C(7) $(2-x, \frac{1}{2}+y, 1-z)$ 3.293(30) Å.

The authors wish to thank Messrs. Tomohiro Sato and Hitoshi Nakai, Shionogi Research Laboratory, for providing the crystals and their technical assistance. K. O. is grateful to Professor Mario Nardelli, University of Parma, for compiling his program. Professor Kenneth N. Trueblood, University of California, helped K. O. in installing his program and in analyzing the thermal motions.

References

- 1) K. Okada and H. Koyama, *J. Appl. Crystallogr.*, **24**, 1067 (1991).
- 2) "International Tables for X-Ray Crystallography," Kynoch Press, Birmingham (1974), Vol. IV, pp. 99–102, 149.
- 3) Additional material deposited as Document No. 67002 at the Office of the Editor of Bull. Chem. Soc. Jpn. comprised hydrogen atom coordinates, thermal parameters, remaining bond lengths, best least-squares planes, and intermolecular distances.
- 4) D. Cremer and J. A. Pople, *J. Am. Chem. Soc.*, **97**, 1354 (1975).
- 5) M. Nardelli, *Acta Crystallogr., Sect. C*, **C39**, 1141 (1983).
- 6) J. D. Dunitz, *Pure Appl. Chem.*, **25**, 495 (1971).
- 7) The type I atom having one achiral H atom is bonded to one intra- and one extra-annular H atoms. A type II atom has one axial and one equatorial extra-annular H atoms.
- 8) H.-C. Mez, G. Rist, O. Ermer, L. Lorenc, J. Kalvoda, and M. L. Mihailovic, *Helv. Chim. Acta*, **59**, 1273 (1976).
- 9) A. T. McPhail, K. D. Onan, and P. M. Gross, *J. Chem. Soc., Perkin Trans. 2*, **1975**, 1798.
- 10) G. Appendino, G. Chiari, P. Ugliengo, and D. Viterbo, *J. Chem. Soc., Perkin Trans. 2*, **1987**, 215.
- 11) U. Rychlewska, *J. Chem. Soc., Perkin Trans. 2*, **1981**, 660.
- 12) V. Schomaker and K. N. Trueblood, *Acta Crystallogr., Sect. B*, **B24**, 63 (1968).
- 13) K. N. Trueblood, *Acta Crystallogr., Sect. A*, **A34**, 950 (1978).
- 14) J. D. Dunitz and D. N. J. White, *Acta Crystallogr., Sect. A*, **A29**, 93 (1973).
- 15) K. N. Trueblood, "THMA14, The computer program for thermal motion analysis including internal torsion," University of California, Los Angeles, USA (1992).
- 16) W. R. Busing and H. A. Levy, *Acta Crystallogr.*, **17**, 142 (1964).
- 17) M. Nardelli, "ROTENER, A Fortran routine for calculating non-bonded potential energy," University of Parma, Parma, Italy (1992).
- 18) J. Gasteiger and M. Marsili, *Tetrahedron*, **36**, 3219 (1980).
- 19) C. K. Johnson, "ORTEP-II, A Fortran thermal-ellipsoid plot program for crystal structure illustrations," ORNL-5138 (Third Rev. of ORNL-3794), Oak Ridge National Laboratory, Oak Ridge, Tennessee, USA (1976).